composition$25SiO_2–25Pb_3O_4–(50–x)B_2O_3–xGd_2O_3$ where x = 1, 2, 3 and 4mol % were extensivelystudied.

2. Experimental procedures

Pure raw materials of Pb_3O_4, Si_2O, H_3BO_3, and Gd_2O_3were mixed thoroughly and melted at a temperature range of 1000 °C in high purity porcelain crucible to produce glass system in a chemical formula$25SiO_2–25Pb_3O_4–(50–x)B_2O_3$-$xGd_2O_3$where x = 1, 2, 3, and 4mol %. The molten was annealed at 350°C for an hour to remove the residual stresses. The amorphous phase of the produced glasses was examined using X-ray diffraction. The density of the glassy samples was measured according to the standard Archimedes principle [14-15] using Xylene as an immersion liquid. Fourier Transform Infrared (FTIR) measurements were carried out by an infrared spectrometer type Jasco FTIR-300E (Japan) in the range of (4000–400 cm-1). IR spectra of powdered samples were obtained in potassium bromide (KBr) pellet. Careful grinding was performed to avoid errors caused by scattering. Computer-aided double-beam spectrophotometer (JASCO corp. v-570, UV/ VIS/NIR, Japan) was used to record the UV-visible absorption spectra on slab plane glass samples. The resolution limit of the spectrophotometer is δλ= 0.1 nm. The accuracy of measuring reflectance and transmittance is ± 0.002 with the incident beam making an angle of 5°±0.1 to the normal of the external slab face. Gamma ray mass attenuation coefficients are obtained using Phy-X/PSD computer software. The effective removal cross section of the fast neutrons was calculated through the Phy-X/PSD software and the below mixture rule [16-18]

$$\Sigma_R = \Sigma_i W_i \left(\frac{\Sigma_R}{\rho}\right)_i$$

where, $W_i$and $\left(\frac{\Sigma_R}{\rho}\right)_i$are the partial density and massremoval cross section of the ithconstituents.

For thermal neutron, the total macroscopic cross section was calculated using [16-18]

$$\sigma_T = N_A \rho \sum_i \frac{W_i}{M_i}(\sigma_c + \sigma_{in} + \sigma_a)$$

where,N_A, ρ, W_i, and M_i are the Avogadro's number, density, ith element mass fraction, and ithelement atomic mass and σ_c, σ_{in}, and σ_a are the coherent scattering, incoherent scattering, and absorption cross sections of thermal neutron.

3. Results and discussion

X-ray diffraction (XRD) pattern as shown in **Figure 1**showed that there are neither discrete nor sharp peaks, but there is only one broad halo.The absence of Bragg's peak indicates that the studied materials have an amorphous nature.

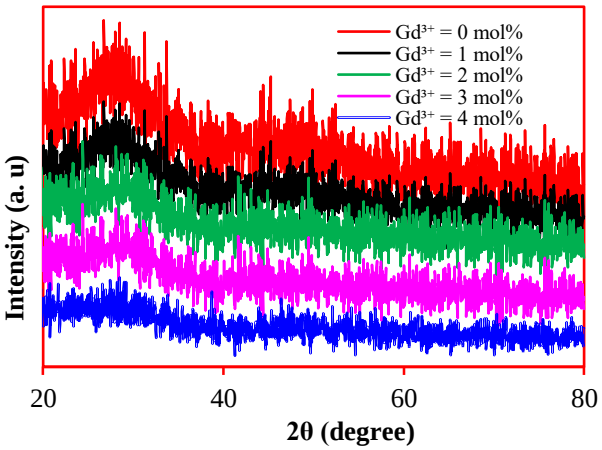

Fig. 1. The amporphicity check of the studied samples

Two regions were found in the density and molar volume behavior as shown in **Figure 2**. In the first region up to 1 mol% of gadolinium, the density increases and the molar volume decreases, while in the second region a reduction in density and augmentation in molar volume was observed.In the first region, the density augmentation is due to the replacement of the B^{3+} ion with the lower atomic number by Gd^{3+} with the larger atomic number. While, the reduction in molar volume resulted from filling the interstitial spaces with the inserted Gd^{3+} ion in the studied glass network, which increases the tightness of the packing inside it. The second point, the density reduction after 1 mol% of Gd^{3+}, despite being heavier than boron, stems from the structural units of the incorporated oxides, which leads to the formation of silicon and boron threefold rings instead of fourfold ones. Combining $Gd^{3+}$and Pb^{2+}transforms fourfold silicon and boron to threefold i.e., SiO_4 to SiO_3 and BO_4 to BO_3 causing the creation of non-bridging oxygen, forming an open structure. This was evident in the increase in the molar volume beyond 1 mol% of Gd^{3+}.

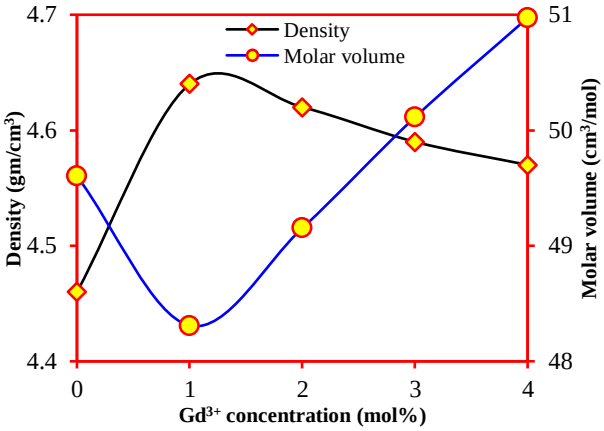

Fig. 2. Variation of density and molar volume with gadolinium oxide

The behavior of both mean boron-boron separation (MB-BS) and mean silicon-silicon separation (MS-SS), as shown in **Figure 3**, confirmed the change of the produced glass structure from tight to open with the change in Gd^{3+} concentration, which confirms the obtained molar volume results.

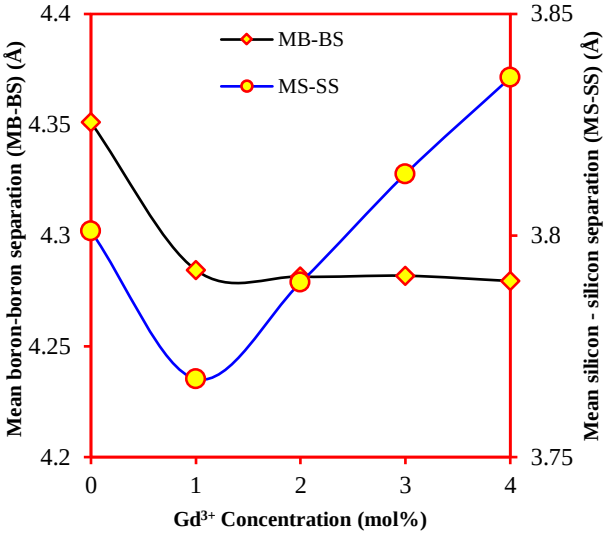

Fig. 3. Variation of mean boron-boron separation and mean silicon-silicon separation as a function in Gd^{3+} concentration

Oxygen packing density OPD and packing density PDexplore precisely the tightness inside the glass network. The values of OPD and PDare estimated using the following equation [19-21]

$$OPD = \frac{\rho}{M} \times n$$

$$PD = \frac{\rho}{M} \sum_i x_i V_i$$

where, n is the number of oxygen atoms per formula unit,x_i the mol fraction, and V_i the packing factor

$$V_i = \frac{4\pi N_A}{3}(br_A^3 + cr_B^3)$$

where, N_A and$r_A$and r_B are the Avogadro's number and the ionic radii of the cation and the anion, respectively.

The augmentation of both oxygen packing density and packing density up to 1 mol% of Gd^{3+} and as observed in **Figure 4** indicates the tight packing of the considered lead borosilicate network and decreases the disorder degree i.e., formation of SiO_4 and BO_4 units, which in perfect agreement with molar volume trend and mean boron – boron separation and mean silicon – silicon separation. Beyond up 1 mol% of Gd^{3+}, the combined Pb^{2+} and Gd^{3+} convert both SiO_3 to SiO_4 and BO_3 to BO_4 (this is clearly observed in the FTIR results) brought a reduction in oxygen packing density and packing density, which means loosely packing of the considered glasses.

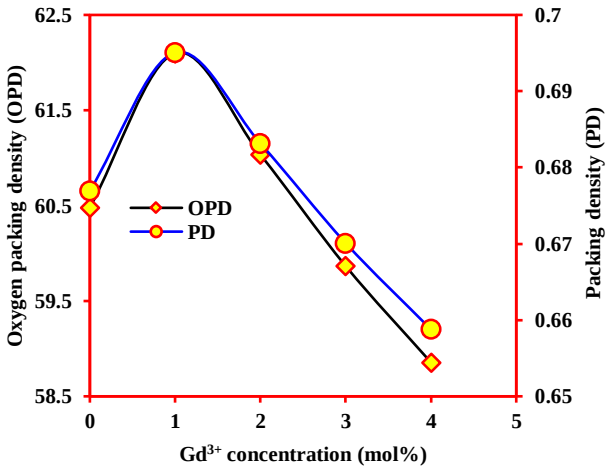

Fig. 4. Variation of both oxygen packing density and packing density with Gd^{3+}ions content

As observed from FTIR spectra displayed in**Figure 5** increase of Gd^{3+}ions content modifies thecharacteristic of IR bands. Four bands were located throughout the studiedFTIR wavenumber range 400-1600 cm^{-1}in the regions 456-466, 697-699, 955 961, and 1341-1342 cm^{-1}. The bands of O-B-Ocovalent and Pb–O bond vibrations are observed between 456 and 466 cm-1[22-23].Also, the B-O-Si stretching, the Si-O-Si symmetric stretching of bridging oxygen atoms between the tetrahedral, and O-Si-O bending bands arise around this range [24-25]. Theobserved bands in the region 697-699$cm^{-1}$are due to B–O–B bond-bending vibrations from pentaborate groups [26-27]. In the region of 955–961 cm^{-1}, bands appeared due to the stretching of B-O bond in tetrahedral BO_4units, which are the vibrations of tetra borate (tri borate and pentaborate) groups of BO_4 units [28-29]. Bands in the region 1180–1520 cm^{-1} are usually attributed to B–O bond stretching of trigonal BO3 units [23, 28].

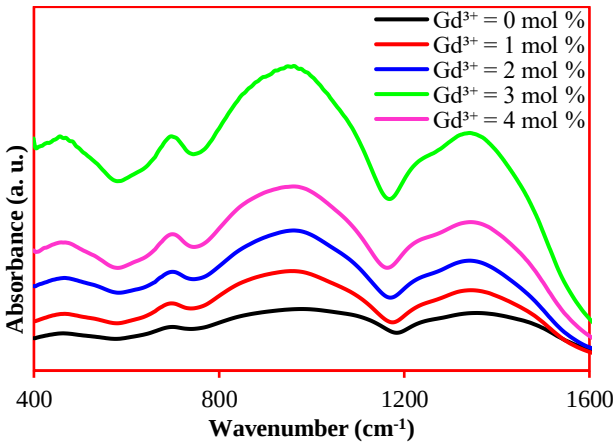

Fig. 5.FTIR spectra of the considered glasses

The optical transmission spectra of the considered glasses are shown in **Figure 6**. The absence of sharp

edges in the optical spectra verifies the amorphous phase of the studied glasses.

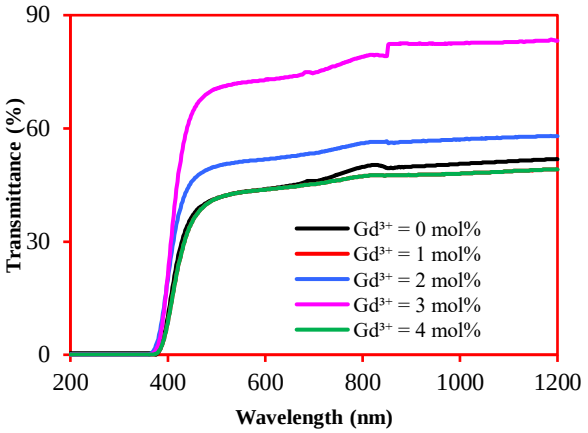

Fig. 6. Optical transmission spectra of the studied glasses

The cutoff wavelength values in the spectra reflect a large transmission window. A reduction in the transmission spectra with the increase of the Gd^{3+} content at 1 mol% was observed and an augmentation beyond this point up to 3mol % of Gd^{3+}. The observed reduction in transmittance spectra at 1 mol% of Gd^{3+} is due to the replacement of B^{3+} with molecular mass less than that of Gd^{3+}, which causes an attenuation of the incident light. The increase of the transmittance spectra at 2 then 3 mol% Gd^{3+} is attributed to an increase in the concentration of highly coordinated Pb^{+2} in PbO_4 bipyramids at the expense of B_4(Pb) units

The plot of $(\alpha h\nu)^{1/2}$ versus photon energy $h\nu$ (Tauc's plot) was conducted to estimate the indirect optical band gapE_g[5]. The lack of crystalline long-range order in glassy materials is associated with a tailing of the density of states into the normally forbidden energy band. It occurs when the energy of the incident photon is less than the band gap then; the increase in the absorption coefficient is followed by an exponential decay of density localized states into the gap. The width of these band tails is known as the Urbach energyΔE. To calculate the Urbach energy ΔE according to Urbach and Tauc model, the following relation is valid [30-35]

$$\ln \alpha(\nu) = \ln \alpha_o + \left(\frac{h\nu}{\Delta E}\right)$$

The obtained values of optical band gap and Urbach energy were given as a function in Gd_2O_3 as shown in **Figure 7**.

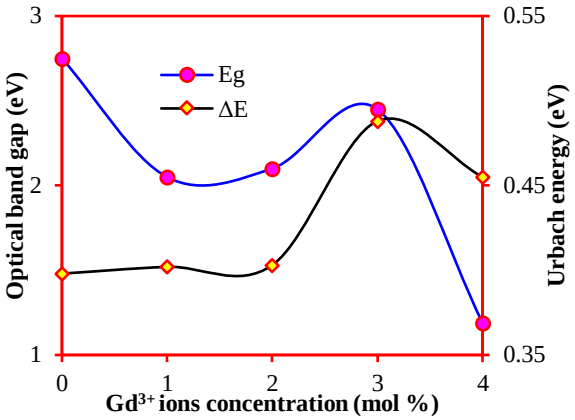

Fig. 7. Variation of optical band gap and Urbach energy as a function of Gd^{3+}content

The optical band gap decrement at 1 mol % of $Gd^{3+}$is attributed to the formation of band tails on both conduction and valence bands. The augmentation of the band gapup to 3 mol % of Gd^{3+}wasattributed to the movement of electron density away from the Pb^{+2} ions, the densest ion in the present structure, (nephelauxetic effect). Urbach energy, which corresponds to the width of localized states, is used to characterize the degree of disorder in amorphous and crystalline systems. Materials with larger Urbach energy would have greater tendency to convert weak bonds into defects. The values of ΔE of the present glass system are shown in **Figure 7**. It is clear that the band width values increase with increasing Gd^{3+}contentup to 3 mol%, then decrease. The trend of the increase in ΔE may be attributed to the increase in the degree of disorder which causes more defects or localized states in the band gap.

In the mass attenuation coefficients behavior of Gd^{3+} free sample as shown in **Figure 8a** sharp a reduction from 1 keV to 300keVand meager one from 300keV to 13 MeV are observed followed by slight increase in the rest of the studied energies spectrum. The highest values of the mass attenuation coefficients in the low energy region from 1 keV to 300 Kev due to the domination of the photoelectric effect, which its cross section τ/ρstrong depends on the atomic number of the shielding materials Z, $\tau/\rho \propto Z^m$, where $m = 3.6 - 5.3$[36-37]. The sharpest reduction in mass attenuation coefficients with the gamma ray energy augmentation attributed to the proportional of the photoelectric cross section τ/ρ with E^{-n}, where $n = 2.5 - 3.5$ [36-37]. The emerged jump in the mass attenuation coefficients 100keVare attributed to the absorption of gamma photons in K-edge of Pb. The meager diminution in mass attenuation coefficients from 300 keV to 13 MeV arose due to the Compton Effect interaction, in which its cross section σ/ρ is proportional to E^{-1} [36-37].

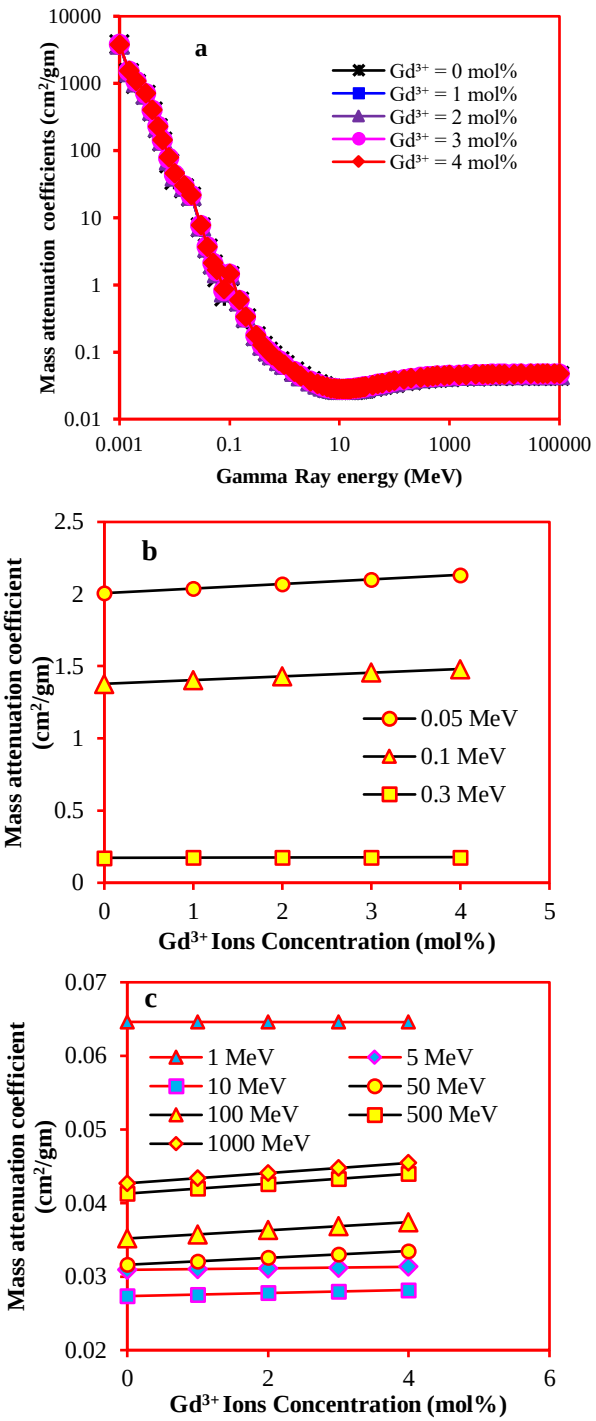

Fig. 8. a) variation of mass attenuation coefficient as a function in gamma ray energy and mass attenuation coefficient as a function in Gd^{3+} ions b) for low energy and c) for high energy

The low values of mass attenuation coefficients in Compton region are due to the weakly depends of its cross section σ/ρon the atomic structure of the shielding materials, $\sigma/\rho \propto Z$. The re-increase in the mass attenuation coefficients beyond 13 MeV attributed to the dependency of the pair production cross section on Z^2, $\kappa/\rho \propto Z^2$[36-38]. With Gd^{3+} ions insertion into the considered lead borosilicateglass;mass attenuation coefficient is increased reflecting its effective role to attenuate gamma ray as shown in **Figure 8b** (low energy gamma rays) and c (intermediate and high gamma rays).

The density variation with the change in the Gd^{3+} ions concentration affected the behavior of fast neutron removal cross sections as shown in **Figure 9**.

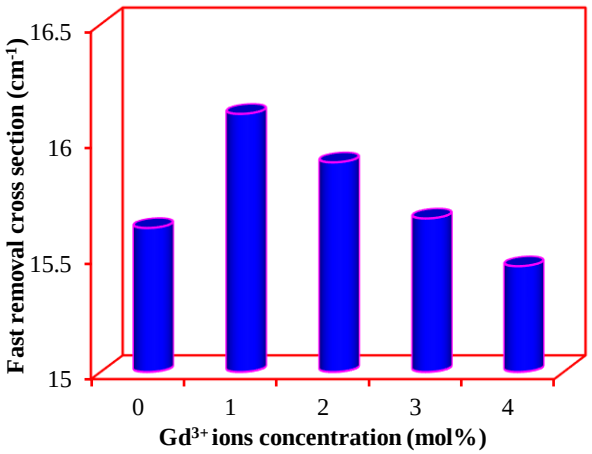

Fig. 9. Fast neutron cross section of the considered glasses

Increasing Gd^{3+} ions concentrations showed a significant effect on thermal neutrons cross section, as gadolinium has a large thermal neutron cross section is 49700 barns.**Figure 10**shows the strong impact of Gd^{3+} ions on the attenuation of thermal neutrons reflecting its efficiency as thermal neutrons attenuator.

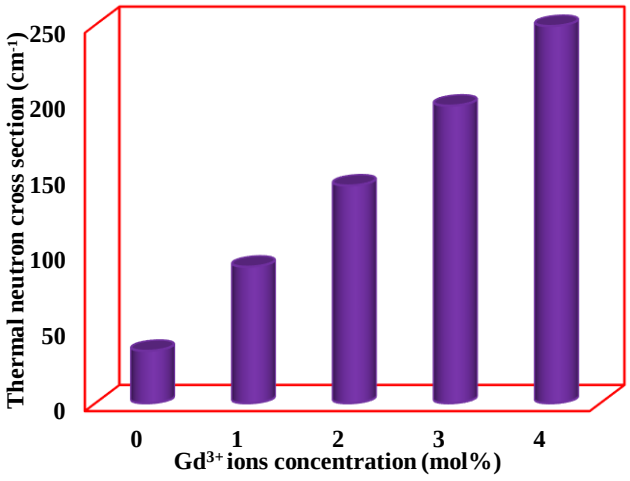

Conclusions

The structural, optical, and radiation attenuation role of Gd^{3+} ions in lead borosilicate glasses were investigated. The density, molar volume, and FTIR results confirm the assumption that the Gd^{3+} ions played a dual role, modifiers and

formers, in the present lead borosilicate glasses. The optical transmittance spectra of the studied glasses show a high transmission in the visible region. On the other hand, a strong absorption was observed in the UV-region.The optical band gap lies in the range of amorphous semiconductor. Gd^{3+} ions enhance the attenuation ability of gamma ray, fast neutrons and thermal neutrons. The study output confirms that Gd^{3+} ion has an effective optical and attenuating role in the lead borosilicate glass network, which enables it to become a distinguished choice in optical applications and nuclear shields.

Conflicts of interest

The authors have no conflict of interest to declare related to the content of the article.

Reference

[1] Farag, M. A., Abd-Allah, K., Turky, G., Alokr, M. M., Optical and upconversion properties of Nd doped lead borate barium glass system. Nature and Science, 13(5) (2015).

[2] Saeed, Aly,Elbashar, Y. H., and El shazly, R. M., Optical properties of high density barium borate glass for gamma ray shielding applications.Optical and Quantum Electronics, 48(1) 1-10 (2016).

[3] Ruengsri, S., Insiripong, S., Sangwaranatee, N., Kaewkhao, J., Development of barium borosilicate glasses for radiation shielding materials using rice husk ash as a silica source. Progress in Nuclear Energy, 83, 99-104 (2019).

[4] Hafez, Shaimaa, El-Kameesy, S. U., Eissa, M. M., Elshazly, R. M.,El Fawkhry, M. K., Saeed, Aly, The effect of boron and titanium addition on the behavior of steel alloys of base composition AISI304Mo as a nuclear radiation shielding material.Arab Journal of Nuclear Sciences and Applications, 52(4), 36-44(2019).

[5] Saeed, Aly, El shazly, R. M., Elbashar, Y. H., Abou El-azm, A. M., Comsan, M. N. H., El-Okr, M. M., and Kansouh, W. A., Glass materials in nuclear technology for gamma ray and neutron radiation shielding: a review. Nonlinear Optics, Quantum Optics,53,107–159 (2020).

[6] Eid, A. M., Farag, M. A.,Abd El-Rahman, K. A., El-Okr, M. M., Ultrasonic study on complex glass system doped with erbium oxide. Journal of Materials Research, 31(04), 495-505 (2016).

[7] Adel, A., Farag, M., El-Okr, M., Elrasasi, T., El-Mansy, M., Preparation and characterization of phosphate glasses co-doped with rare earth ions. Egyptian Journal of Chemistry, 63(5), 1955 – 1964 (2020).

[8] Vani, P., Vinitha, G., Sayyed, M.I., AlShammari, Maha M., Manikandan, N., Effect of rare earth dopants on the radiation shielding properties of barium tellurite glasses.Nuclear Engineering and Technology, 53, 4106-4113 (2021).

[9] Kliava, J., Edelman, I. S., Potseluyko, A. M., Petrakovskaja, E. A., Berger, R., Bruckental, I., Yeshurun, Y., Malakhovskii, A. V., and Zarubina, T. V.,Magnetic and optical properties and electron paramagnetic resonance of gadolinium-containing oxide glasses.Journalof Physics: Condensed Matter, 15, 6671–6681(2003).

[10] Zagrai, M., Unguresan, M., Rada, S., Zhang, J., Pica, M., Culea, E.,Local structure in gadolinium-lead-borate glasses and glass-ceramics.Journal of Non-Crystalline Solids, 546, 120259(2020).

[11] Kliava, Janis, Malakhovskii, Alexander,Edelman, Irina, Zarubina, Tat'jana, Petrovskii, Gurii, Bruckental, Yishay, and Yeshurun, Yosef,Unusual magnetic transitions and nature of magnetic resonance spectra in oxide glasses containing gadolinium. Physical Review B, 71, 104406 (2005).

[12] Rada, S., Rada, M., Erhan, R., Bodnarchuk, V., Tudoran, BarbuL., Culea, E.,Hetertogeneities in the silver oxide-lead-germanate glasses. Journal of Alloys and Compounds, 770, 395–404(2019).

[13] Shamshad, L., Rooh, G., Limkitjaroenporn, P., Srisittipokakun, N., Chaiphaksa, W., Kim, H.J., Kaewkhao, J., A comparative study of gadolinium based oxide and oxyfluoride glasses as low energy radiation shielding materials.Progress in Nuclear Energy, 97, 53-59 (2017).

[14] Elbashar, Y., Saeed, Aly, Rayan, D. A., Prism method of studying the refractive index for zinc borate sodium glass doped neodymium oxideJournal of Ceramic Processing Research17(6), 532-536 (2016).

[15] Saeed, Aly and Abu-raia, W. A., Silicone rubber composite reinforced by bismuth tungsten oxide as an effective gamma ray protective materials.Journal of Polymer Research,29(5), 208 (2022).

[16] Ali, NohaM., Saeed, Aly, El Shazly, R. M., Al-Fiki, S. A., Eissa, M. M., Elkameesy, S. U., Attenuation effectiveness of double phase stainless steel alloys for fusion reactor system. IOP Conf. Series: Materials Science and Engineering, 956, 012008(2020).

[17] El-Gharbawy, S., Saudi, H., Said, M., Farag, M., Hassaan, M., Structural, Optical, and Shielding Studies of Some Sb Glasses based Egyptian nano-Rock Wool, Egyptian Journal of Chemistry, (Accepted) (2022).

[18] Rammah, Y. S., Olarinoye, I. O.,El-Agawany, F. I., Ahmed, Emad M., and Salem, Waheed M., Influence of Sm_2O_3 content on photon and fast neutron interaction parameters of zinc-tellurite glasses, Radiation Physics and Chemistry, 192, 109914(2022).

[19] Farouk, M., Samir, A., Ibrahim, A., Farag, M. A., Solieman, A., Raman, FTIR Studies and Optical Absorption of Zinc Borate Glasses Containing WO3. Journal of Applied Physics A, 126, 696(2020)

[20] Gautam, Chandkiram, Yadav, Avadhesh Kumar, and Singh, Arbind Kumar, A review on infrared spectroscopy of borate glasses with effects of different additives".ISRN Ceramics, 2012, 428497(2012).

[21] Ibrahim, A., Farag, M.A., Sadeq, M.S., Towards highly transparent tungsten zinc sodium borate glasses for radiation shielding purposes. Ceramics International, 48(9), 12079-12090, (2022)

[22] Saeed, Aly,Elbashar,Y. H., andElKameesy, S. U., A novel barium borate glasses for optical applications. Silicon, 10, 569–574(2018).

[23] Saeed, Aly,Elbashar, Y. H., andElKameesy, S. U., Optical spectroscopic analysis of high density lead borosilicate glasses.Silicon,10, 185 – 189 (2018).

[24] El-Batal, A. M.,Farag, M. A., El-Okr, M. M., andSaeed,Aly, Influence of the addition of two transition metal ions to sodium zinc borophosphate glasses for optical applications. Egyptian Journal of Chemistry, 64(12), 6953 – 6958 (2020).

[25] El-Batal, A. M., Saeed, Aly, Hendawy, N., El-Okr, M. M., and El-Mansy, M.K., Influence of Mo or/and Co ions on the structural and optical properties of phosphate zinc lithium glasses. Journal of Non-Crystalline Solids, 559, 120678, (2021).

[26] Bootjomchai, C.,Laopaiboon, J.,Yenchai,C.,Laopaiboon, R., Gamma-ray shielding and structural properties of barium-bismuth-borosilicate glasses,Radiation Physicsand Chemistry, 81(7), 785–790(2012).

[27] Kurudirek, M.,Chutithanapanon, N.,Laopaiboon, R.,Yenchai, C.,Bootjomchai, C.,Effect of Bi_2O_3 on gamma ray shielding and structural properties of borosilicate glasses recycled from high pressure sodium lamp glass.Journal of Alloys and Compounds, 745, 355–364(2018).

[28] Sreekanth,Chakradhar R. P., Ramesh, K. P., Rao, J. L., Ramakrishna, J., Mixed alkali effect in borate glasses—EPR and optical absorption studies in $xNa_2O–(30-x)K_2O–70B_2O_3$ glasses doped withMn2+. Journal of Chemistry and Physics solids, 64,641–650 (2003).

[29] Alhodaib, Aiyeshah, Ibrahim, Omnia,Abd El All, Suzy, andEzzeldin,Fatthy, Effect of rare-earth ions on the optical and PL properties of novel borosilicate glass developed from agricultural waste,Materials,14, 5607 (2021).

[30] Saeed, Aly, Sobaih, S., Abu-raia, W. A., Abdelghany, A., and Heikal, Sh., "Novel Er^{3+} doped heavy metals oxyfluorophosphate glass as a blue emitter", Optical and Quantum Electronics 53 (2021) 482

[31] Saeed, Aly, Farag, M. A., andAbu-raia,W. A., Er^{3+} ion doped low phonon energy glass as a white light emitter.Egyptian Journal of Solids,43,97 – 110 (2021).

[32] Saeed, Aly,Elbashar, Y. H., andElKameesy, S. U., Study of gamma ray attenuation of high-density bismuth silicate glass for shielding applications.Research Journal of Pharmaceutical, Biological and Chemical Sciences,6(4), 1830 – 1837(2015).

[33] Elbashar, Y. H., and Saeed, Aly,Computational spectroscopic analysis by using Clausius–Mossotti method for sodium borate glass doped neodymium oxide. Research Journal of Pharmaceutical, Biological and Chemical Sciences,6(5), 230 – 326 (2015).

[34] El-Batal, A. M., Saeed, Aly, Hendawy, N., El-Okr, M. M., and El-Mansy, M.K., Influence of Mo or/and Co ions on the structural and optical properties of phosphate zinc lithium glasses. Journal of Non-Crystalline Solids, 559, 120678, (2021).

[35] Abu raia, W. A., Aloraini, D. A., El Khateeb, S. A. &Saeed, Aly, Ni ions doped oxyflourophosphate glass as a triple ultraviolet–visible–near infrared broad bandpass optical filter.Scientific reports, 12(1), 16024 (2022).

[36] Eissa, M. M., El-Hossary, F. M., El-Kameesy, S. U., Saeed, Aly, Abd Elmoula, Al-Zahraa A., Al Shelkamy, Samah A., Mechanical and gamma ray attenuation properties of N316L steel treated by RF plasma as a nuclear material.Arab Journal of Nuclear Sciences and Applications, 52(2), 7-12 (2019).

[37] El-Kameesy, S. U., El-Hossary, F. M., M. M., Eissa, Abd El-Moula, A. A., Al-Shelkamy, Samah A., and Saeed, A., Radiation shielding, mechanical and tribological properties of treated AISI304L using H_2/N_2 rf plasma. Journal of Physics: Conf. Series, 1253, 012034(2019).

[38] Teresa, P. Evangelin, Naseer, K. A.,Marimuthu,Alavian, K., Hoda, and Sayyed, M. I., Influence of modifiers on the physical, structural, elastic and radiation shielding competence of Dy^{3+} ions doped Alkali boro-tellurite glasses. Radiation Physics and Chemistry, 189, 109741(2021).